This article has been accepted for publication in IEEE Transactions on Intelligent Vehicles. This is the author's version which has not been fully edited and content may change prior to final publication. Citation information: DOI 10.1109/TIV.2022.3225466

Secrecy Performance for RIS-based Integrated Satellite Vehicle Networks with A UAV Relay and MRC Eavesdropping

Feng Zhou, Xingwang Li, *Senior Member*, *IEEE*, Mamoun Alazab, *Senior Member*, *IEEE*, Rutvij H. Jhaveri, *Senior Member*, *IEEE*, and Kefeng Guo

***Abstract*—This work investigates the secrecy issues for the secrecy reconfigurable intelligent surface-based integrated satellite unmanned aerial vehicle (UAV) relay networks with multiple vehicle eavesdroppers. Particularly, the maximal ratio combining (MRC) eavesdropping is utilized to overhear the legitimate signal information. The UAV is applied to forward the legitimate signal to the destination user. Reconfigurable intelligent surface is applied to ensure the transmission. Relied on the proposed secrecy system model and MRC eavesdropping scheme, this paper gets the detailed investigations for the secrecy outage probability (SOP) through the whole signal-to-noise ratios (SNRs) to valuate the effects of important parameters on the SOP. Moreover, to achieve the further impacts of main parameters on the SOP at high SNRs, the approximate analysis for the SOP is also gotten together with the secrecy diversity order (SDO) and secrecy coding gain (SCG). At last, several typical Monte Carlo (MC) results are obtained to present the rightness of obtained theoretical analysis.**

***Index Terms*—Reconfigurable intelligent surface (RIS), integrated satellite-unmanned aerial vehicle (UAV)-relay networks, maximal ratio combining (MRC) eavesdropping scheme, secrecy outage probability.**

I. Introduction

WITH the rapid development of the wireless communication, high data transmission rate, high energy efficiency and high secrecy security are the inherent characters for the wireless communication networks [1]–[4]. On this foundation, satellite communication (SatCom) networks come to our sight, for it can satisfy the high data transmission rate, and is regarded as the major part of the next generation networks [5]–[8] which come from the academic and industrial societies [9]–[11]. In fact, satellite are envisioned to serve billions of terrestrial and flying devices world wide to fulfill the ever-increasing demands of data acquisition and dissemination [12], [13]. However, as the inherent characters for the SatCom, it was a little far from the ground user, thus the terrestrial relay or unmanned-aerial-vehicle (UAV) is used to fulfill this shortage which worked as the forward relay to re-transmit the signal of the source satellite [14]–[16]. When using the terrestrial relay, relay selection, secrecy problem and the other issues have been solved [17]–[21]. In addition, the UAV also plays the important role when forwarding the signals. By both utilizing the superiorities of the SatCom and the UAV systems, the integrated satellite-UAV-relay networks (ISUAVRNs) appear, which have been considered as the important part of the next communication networks [22], [23].

A. Related Works

ISUAVRNs have been the popular topic these years [24], [25] researched the beamforming and performance for the ISUAVRNs, particularly for the internet of things (IoT) networks. In [26], the authors proposed a dynamic trajectory optimization method for the ISUAVRNs. In [27], the authors researched the physical layer security (PLS) for the cybertwin-enabled ISUAVRNs, moreover, two corresponding beamforming optimization approaches are proposed to enhance the PLS. In [28], the authors studied the power optimization scheme for the ISUAVRNs.

As mentioned before, high energy efficiency is a requirement for the next wireless communication networks. To fulfill this goal, reconfigurable intelligent surfaces (RISs) come to our sights, which have been considered as the hopeful method to satisfy this [29]–[33]. RISs come from the human-created surfaces of electromagnetic (EM) material which was easily electronically handled by electronics tools [34]–[37]. [38] studied the outage probability (OP) for the UAV communication systems with the help of RIS, particularly, the deep

This work was supported by the National Science Foundation of China under Grants 62001517 and 61673108, in part by the National Postdoctoral Program for Innovative Talents under Grant BX20200101, in part by the Key Scientific Research Projects of Higher Education Institutions in Henan Province under Grant 23B510001, in part by the Guangdong Basic and Applied Basic Research Foundation with grant number 2022A1515010999, in part by the Science and Technology Program of Guangzhou with grant number 202201011850, and in part by the Scientific Research Project of Education Department of Guangdong with grant number 2021KCXTD061, also in part by the Major Basic Research Project of the Natural Science Foundation of the Jiangsu Higher Education Institutions under grant number 19KJA110002, Supported by the Yancheng Institute of Technology High-level Talent Research Initiation Project under grant number XJR2022001.

F. Zhou is with the School of Information Technology, Yancheng Institute of Technology, Yancheng 224051, China (e-mail: zfycit@ycit.edu.cn).

X. Li is the School of Physics and Electronic Information Engineering, Henan Polytechnic University, Jiaozuo, 454000, China (e-mail: lixingwangbupt@gmail.com).

M. Alazab, is with the College of Engineering, IT and Environment at Charles Darwin University, Casuarina, NT 0810, Australia (e-mail: alazab.m@ieee.org).

R. H. Jhaveri is with the Department of Computer Science and Engineering, School of Technology, Pandit Deendayal Energy University, Gandhinagar 382007, India (e-mail: rutvij.jhaveri@sot.pdpu.ac.in).

K. Guo is with the School of Space Information, Space Engineering University, Beijing 101407, China (e-mail: guokefeng.cool@163.com).

The corresponding author is Kefeng Guo (email: guokefeng.cool@163.com), and the co-corresponding author is Rutvij H. Jhaveri (email: rutvij.jhaveri@sot.pdpu.ac.in).

investigation for the OP was further obtained. [39] researched the performance for the RIS-aided UAV-based vehicular communication system along with multiple non-identical interference. [40] investigated the optimization method for the RIS-aided UAV network by utilizing the deep reinforcement learning optimization method. In [41], the authors proposed a transmit power minimization method for the UAV-assisted RIS hetnets. [42] researched the effects of RIS and UAV relay on the ISUAVRNs, especially, a high altitude platform (HAP) was further utilized. In [43], the effects of the non-ideal hardware and RIS were analyzed for the UAV-assisted ISUAVRNs, particularly, the deep investigations for the OP were further researched. The authors in [44], [45], the authors studied the effective capacity and secrecy performance for the simultaneously transmitting and reflecting RIS networks.

B. Motivations

Also as mentioned before, high security is the other demand for the next wireless communication networks (NWCNs). Thus, it is essential to study the secure issue for the NWCNs, particularly for the ISUAVRNs [46]–[50]. Different from the traditional method, PLS is considered to be the wishing method to analyze the secure problem. In [50], the authors concluded the whole problems for the SatComs. [51] studied the secrecy outage probability (SOP) for the non-orthogonal multiple access (NOMA)-aided cognitive ISUAVRNs, particularly, the SOP was detailedly investigated, furthermore, the secrecy diversity order (SDO) and secrecy coding gain (SCG) by utilizing opportunistic selection scheme was researched. [52] studied the SOP for the integrated satellite terrestrial networks (ISTNs) by applying a threshold-based selection. In [53], [54], the authors proposed an optimization method for the secrecy problem which was suit for the cognitive ISTNs. The proposed optimization method is also fit for the ISUAVRNs. In [55], the authors also proposed an efficient optimization method for the ISTNs. The secrecy problems for RIS-based UAV in the published works were shown in [56]–[58]. [56] developed an efficient secure optimization algorithm for the RIS-based UAV systems. [57] studied the secrecy transmission issue in the millimeter-wave (mmWave) network in the presence of a UAV and a reconfigurable intelligent surface (RIS) with imperfect channel state information (CSI). [58] studied the secure issue for the RIS-based system, where multiple UAV eavesdroppers wanted to steal the legitimate information. However, there is few published papers researching the secure problems for the RIS-aided ISUAVRNs, especially for the maximal ratio combining (MRC) eavesdropping scheme, which motivates our paper.

C. The Contributions of This Paper

Motivated by the former works, by taking the RIS and UAV into our sight, we consider an ISUAVRN, where MRC combining scheme is further used to get better eavesdropping performance. Particularly, the major contributions of the considered system are presented as:

- Taking RIS and UAV-relay into the scene, we illustrate a structure of the ISUAVRN, where multiple vehicle eavesdroppers, a UAV relay, a satellite and a destination are considered. Moreover, decode and forward (DF) scheme is utilized in the UAV relay to help the satellite to transmit the legitimate signals. In addition, multiple vehicle eavesdroppers want to overhear the legitimate information, thus they both overhear the satellite's signals and the UAV's signals. At last, to get best eavesdropping performance, MRC combining scheme is utilized among the vehicle eavesdroppers.
- To achieve the best secrecy performance, RIS technology is used for the considered system. Upon the considered network model, the total SOP expressions are obtained. By utilizing these expressions, the impacts of major system parameters are further derived. The results show that the SOP is mainly judged by the satellite link.
- Some approximate investigations are given to valuate the effect of major parameters for high signal-to-noise ratio (SNR) scenario, relied on the above considerations, the SDO and SCG are along derived. The eavesdroppers' number, the power of the eavesdroppers and the channel fading do not have influence on the SDO, they just affect the secrecy coding gain.

The following sections of this work are shown as the following. In Section II, the detailed investigation of the secrecy vehicle model is given. Though Section III, the investigations for the SOP are derived, particularly, the SDO and SCG are further gotten. For Section IV, several meaningful Monte Carlo (MC) computer results are obtained to make sure the rightness of the analytical results. In Section V, the whole summarization of this work is obtained.

Notations: $F_x(\cdot)$ represents cumulative distribution function (CDF) of x. Moreover, $f_x(\cdot)$ is the probability density function (PDF) of x. The acronyms and abbreviations are obtained in Table I.

II. System Illustration

Described in Fig. 1, through the work, this work investigates the down-link ISUAVRN, which contains a satellite (S), a UAV worked as a DF relay (R), a RIS was installed on the tall building to help the transmission for the reason that the target vehicle receiver destination (D)[1] can not communicate with the R directly owing to the obstacles[2]. As the satellite and UAV both have the wide transmission beam coverage, thus, in the open area, multiple vehicle eavesdroppers ($E_j, j \in \{1, \ldots, M\}$) want to overhear the legitimate users' signal. In the whole system model, all transmission nodes are considered to have only one antenna[3]. In addition, MRC eavesdropping scheme is utilized among the multiple vehicle eavesdroppers. It will spend two time slots during the total transmission.

[1] The obtained results are also suitable to the scenario that has many legitimate users as a future direction.

[2] As a result of obstacles and other reasons, in this considered system model, the direct transmission link is not considered, which would be investigated in the near future work.

[3] We should know that, even if the nodes in this paper are equipped with only one antenna, the derived theoretical results are also suitable for the scenario with multiple antennas in the presence of beamforming technology.

TABLE I
ACRONYMS AND ABBREVIATIONS

Acronym	Definition
UAV	unmanned aerial vehicle
MRC	maximal ration combining
SOP	secrecy outage probability
SNR	signal-to-noise ratio
SDO	secrecy diversity order
SCG	secrecy coding gain
MC	Monte Carlo
SatCom	satellite communication
ISUAVRNs	integrated satellite-UAV-relay networks
IoT	internet of things
PLS	physical layer security
RIS	reconfigurable intelligent surfaces
EM	electromagnetic
OP	outage probability
HAP	high altitude platform
NOMA	non-orthogonal multiple access
PDF	probability density function
CDF	cumulative distribution function
SR	shadowed-Rician
AWGN	additive Gaussian white noise
GEO	geosynchronous Earth orbit
TDMA	time division multiple access
FSL	free space loss
LMS	land mobile satellite
LOS	line-of-sight
DF	decode and forward
CSI	channel state information
mmWave	millimeter-wave
DF	decode-and-forward
NWCNs	next wireless communication networks
ISTN	integrated satellite terrestrial networks
LEO	low Earth orbit
MEO	medium Earth orbit
i.i.d	independent identically distributed

A. $S \to R$ Transmission Link

For the first time slot, S transmits the legitimate information signal to R, then the signal obtained at R could be written as

$$y_R(t) = \sqrt{P_S} h_{SR} s(t) + n_R(t), \tag{1}$$

where P_S represents the transmission power of S, $s(t)$ is the target signal from S which satisfies $E\left[|s(t)|^2\right] = 1$, h_{SR} depicts the channel factor between S and R that obeys shadowed-Rician (SR) fading, $n_R(t)$ represents the additive Gaussian white noise (AWGN) at R with modeled as $n_R(t) \sim \mathcal{CN}\left(0, \delta_R^2\right)$.

On the foundation of (1), the derived signal-to-noise ratio

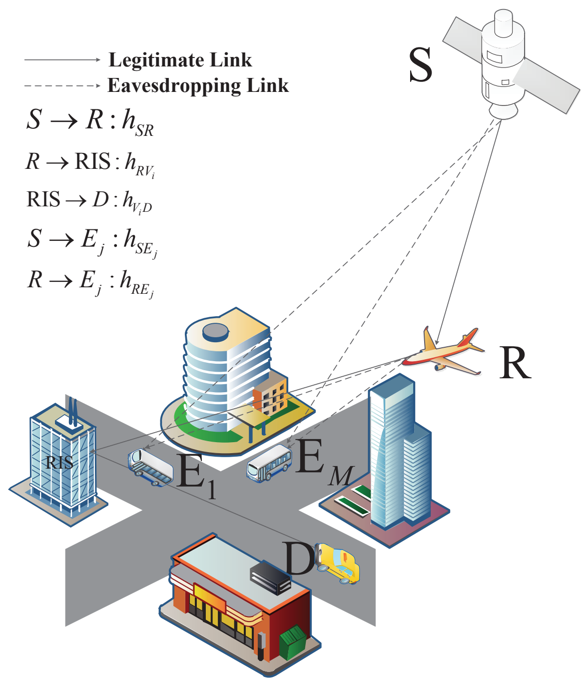

Fig. 1. Description of the secrecy vehicle model.

(SNR) at R is presented as

$$\gamma_{SR} = \frac{P_S |h_{SR}|^2 |s(t)|^2}{|n_R(t)|^2} = \frac{P_S |h_{SR}|^2}{\delta_R^2}. \tag{2}$$

As vehicle eavesdropping exists in this paper, hence the signal obtained at the j-the Eve is given by

$$y_{SE_j}(t) = \sqrt{P_S} h_{SE_j} s(t) + n_{E_j}(t), \tag{3}$$

where h_{SE_j} denotes the channel fading between S and the j-th Eve which undergoes SR fading, $n_{E_j}(t)$ is the AWGN at the j-th vehicle eavesdropper with representation as $n_{E_j}(t) \sim \mathcal{CN}\left(0, \delta_{E_j}^2\right)$.

With the similar way, the obtained SNR at the j-th vehicle E is presented as

$$\gamma_{SE_j} = \frac{P_S \left|h_{SE_j}\right|^2 |s(t)|^2}{\left|n_{E_j}(t)\right|^2} = \frac{P_S \left|h_{SE_j}\right|^2}{\delta_{E_j}^2}. \tag{4}$$

As colluding scheme is utilized in the eavesdroppers, thus the final obtained SNR at vehicle E is presented as

$$\gamma_{SE} = \sum_{j=1}^{M} \gamma_{SE_j}. \tag{5}$$

B. RIS-Assisted $R \to D$ transmission Link

Through the second time slot, R wants to forward the information to vehicle D, owing to the obstacles, R and vehicle D can not communicate with each other directly. Thus, RIS is introduced to help the transmission. So, the obtained signal at vehicle D is written as

$$y_D(t) = \sqrt{P_R}\left[\sum_{i=1}^{N} h_{RV_i} e^{j\varphi_i} h_{V_iD}\right] s(t) + n_D(t), \tag{6}$$

where φ_i represents the phase shift at the RIS's i-th reflecting factor, P_S represents transmission power. h_{RV_i} and h_{V_iD} represent the channel functions given as $h_{RV_i} = \beta_i e^{-\vartheta_i}/\sqrt{L_{RV_i}}$, $h_{V_iD} = \varepsilon_i e^{-\phi_i}/\sqrt{L_{V_iD}}$, respectively. β_i and ε_i are the random variables which obey Rayleigh fading and have a $\sqrt{\pi}/2$ mean and a $(4-\pi)/4$ variance. $L_{RV_i} = 10\log 10\left(l_{RV_i}^{\psi}\right) + A$ and $L_{V_iD} = 10\log 10\left(l_{V_iD}^{\psi}\right) + A$ denote the path loss, A is a fixed value that depends on the transmission frequency and other factors, l_{RV_i} and l_{V_iD} represent the length for the R-RIS and RIS-D transmissions, respectively, ψ denotes the path loss value. $n_D(t)$ represents the AWGN at D obeyed as $n_D(t) \sim \mathcal{CN}\left(0, \delta_D^2\right)$ [43].

From [43], the maximal output signal for the RIS is obtained under the condition $\varphi_i = \vartheta_i + \phi_i$, which is given by

$$y_{RD}(t) = \sqrt{P_R}\left(\underbrace{\sum_{i=1}^{N}\beta_i\varepsilon_i}_{\mathrm{H}}\right)s(t) + n_D(t). \tag{7}$$

Then, by utilizing (7), the maximal SNR at the vehicle D is obtained as

$$\gamma_{RD} = \frac{H^2 P_R}{L_{RV_i} L_{V_iD}\delta_D^2}. \tag{8}$$

As announced before, there are many vehicle Eves in the UAV's transmission beam, then the obtained signal at the j-th vehicle E from the UAV link is derived as

$$y_{RE_j}(t) = \sqrt{P_R} h_{RE_j} s(t) + n_{E_j}(t), \tag{9}$$

where h_{RE_j} denotes the channel fading between R and j-th vehicle E shadowed as Rayleigh fading.

By using (9) and the colluding eavesdropping scheme, the final SNR at vehicle E is denoted as

$$\gamma_{RE} = \sum_{j=1}^{M}\frac{P_R\left|h_{RE_j}\right|^2}{\delta_{E_j}^2} = \sum_{j=1}^{M}\gamma_{RE_j}. \tag{10}$$

For MRC eavesdropping scheme is applied among the vehicle Eves, then the derived SNR for vehicle E is given by

$$\gamma_E = \gamma_{SE} + \gamma_{RE}. \tag{11}$$

As DF mode is utilized at the UAV R, thus the total SNR for the whole link is gotten as

$$\gamma_F = \min\left(\gamma_{SR}, \gamma_{RD}\right). \tag{12}$$

III. Secrecy System Performance Evaluation

During the following section, detailed theoretical results for the SOP are derived. Especially, the closed-form expression is derived based on the system model. In addition, the asymptotic investigations for the SOP are further provided to see the impacts of main parameters on the SOP for high SNR scenario.

A. Preliminaries

Before deriving the detailed SOP analysis, the channel model for the satellite channel, the RIS channel and the terrestrial channel are firstly given.

B. The Satellite Channel

In this considered system model, the geosynchronous Earth orbit (GEO) satellite[4] is chosen for the following investigations. Particularly, the satellite is regarded to have multiple antennas, namely, it has multiple beams along with the time division multiple access (TDMA) scheme[5]. On this foundation, just a user is available for one time slot. $h_V, V \in \{SR, SE_j\}$ denotes the channel factor between the satellite beam center and the UAV/vehicle Eves, which has the presentation as

$$h_V = C_V f_V, \tag{13}$$

where f_V denotes the random SR coefficient, and C_V represents the influences of free space loss (FSL) and antenna pattern with presentation being

$$C_V = \frac{c}{8f\pi^2}\sqrt{\frac{G_V G_R}{d^2 + d_0^2}}, \tag{14}$$

where c is the velocity for the transmission electromagnetic wave, f represents the frequency. d denotes the distance from the satellite' center to the terrestrial relay/eavesdroppers. $d_0 \approx 3.6 \times 10^3 km$. G_V depicts the antenna gain for the UAV relay/vehicle Eves. In addition, G_R is the on-board gain of the satellite.

With the help of [51], G_R is represented as

$$G_R(dB) \simeq \begin{cases} \overline{G}_{\max}, & as\ 0 < \delta < \pi/180 \\ 32 - 25\log(\pi\delta) + 25\log(180), & as\ \pi/180 < \delta < 4\pi/15 \\ -10, & as\ 4\pi/15 < \delta \leq \pi, \end{cases} \tag{15}$$

where $\overline{G}_{\max}$ represents the largest beam effort with δ denoting the angle. By regarding G_V by considering θ_k as the angle. $\overline{\theta}_k$ represents the 3dB angle. Moreover, the gain for the antenna G_V can be shown as [6]

$$G_V \simeq G_{\max}\left(\frac{K_1(u_k)}{2u_k} + 36\frac{K_3(u_k)}{u_k^3}\right), \tag{16}$$

where G_{max} depicts the maximum beam effort, $u_k = 2.07123\sin\theta_k/\sin\overline{\theta}_k$, K_3 and K_1 represent the 1st-kind bessel function of order 3 and 1, respectively. For purpose to obtain the best effort, by regarding $\theta_k \to 0$, the largest gain can be obtained which has a result that $G_V \approx G_{\max}$. Based on the former consideration, we derive $h_V = C_V^{\max} f_V$.

For f_V, the popular SR model appeared in [51], this has been applied when investigating land mobile satellite (LMS) systems [50]. After utilizing [6], f_V could be re-written as $f_V = \overline{f}_V + \widetilde{f}_V$, where $\widetilde{f}_O$ is assumed to undergo independent identically distributed (i.i.d) Rayleigh shadowing, $\overline{f}_V$ represents the issue of line-of-sight (LOS) factor that suffers from i.i.d Nakagami-m fading.

[4]Although in this paper, we take the GEO satellite for an example, the obtained investigations can be also used to the scenario with medium Earth orbit (MEO) and low Earth orbit (LEO) satellites.

[5]TDMA scheme is utilized here to ensure that one satellite beam and one UAV is utilized for a single data transmission time slot.

In addition, the PDF of $\gamma_V = \bar{\gamma}_V |h_V|^2 = \bar{\gamma}_V |C_V^{\max} f_V|^2$ is derived as

$$f_{\gamma_V}(x) = \sum_{k_1=0}^{m_V-1} \frac{\alpha_V (1-m_V)_{k_1} (-\delta_V)^{k_1} x^{k_1}}{(k_1!)^2 \overline{\gamma}_V^{k_1+1} \exp(\Delta_V x)}, \tag{17}$$

where $\overline{\gamma}_V$ denotes the average SNR from S to legitimate vehicle user/vehicle eavesdroppers, $\Delta_V = \frac{\beta_V - \sigma_V}{\overline{\gamma}_V}$, $\alpha_V = \left(\frac{2b_V m_V}{2b_V m_V + \Omega_V}\right)^{m_V} / 2b_V$, $\beta_V = 1/2b_V$, $\delta_V = \frac{\Omega_V}{(2b_V m_V + \Omega_V) 2b_V}$, where $m_V \geq 0$ represents the fading factors, $2b_V$ depicts the power of the multipath factor, moreover Ω_V denotes the power for the LOS factor. It is a popular consideration that, i.e. m_V is regarded as an integer [20]. $(\cdot)_{k_1}$ represents the Pochhammer symbol [59].

Relied on (17), then by using [21], the CDF of γ_V could be derived as

$$F_{\gamma_V}(x) = 1 - \sum_{k_1=0}^{m_V-1} \sum_{t=0}^{k_1} \frac{\alpha_V (1-m_V)_{k_1} (-\delta_V)^{k_1} x^t}{k_1! t! \overline{\gamma}_V^{k_1+1} \Delta_V^{k_1-t+1} \exp(\Delta_V x)}. \tag{18}$$

By [60], the PDF of γ_{SE} could be given by

$$f_{\gamma_{SE}}(x) = \sum_{\xi_1=0}^{m_{SE}-1} \cdots \sum_{\xi_M=0}^{m_{SE}-1} \Xi(M) x^{\Lambda_{SE}-1} \exp(-\Delta_{SE} x), \tag{19}$$

where

$$\Xi(M) \triangleq \prod_{\tau=1}^{M} \varsigma(\xi_\tau) a_{SE}^M \prod_{\ell=1}^{M-1} B\left(\sum_{l=1}^{\ell} \xi_l + \ell, \xi_{l+1} + 1\right),$$

$\Lambda_{SE} \triangleq \sum_{\tau=1}^{M} \xi_\tau + M$, $\varsigma(\xi_\tau) = \frac{(1-m_{SE})_{\xi_\tau} (-\delta_{SE})^{\xi_\tau}}{(\xi_\tau!)^2 \overline{\lambda}_{SE}^{\xi_\tau+1}}$, $\Delta_{SE} = \frac{\beta_{SE} - \alpha_{SE}}{\overline{\lambda}_{SE}}$, $\alpha_{SE} = \left(\frac{2b_{SE} m_{SE}}{2b_{SE} m_{SE} + \Omega_{SE}}\right)^{m_{SE}} / 2b_{SE}$, $\beta_{SE} = 1/2b_{SE}$, $\delta_{SE} = \frac{\Omega_{SE}}{(2b_{SE} m_{SE} + \Omega_{SE}) 2b_{SE}}$ and $B(.,.)$ denotes the Beta function [59].

1) The Terrestrial Channel: From [38], the UAV-RIS-user channel γ_{RD} has the following expression as

$$f_{\gamma_{RD}}(x) \simeq \frac{e^{-\frac{(x - \overline{\gamma}_{RD} s)^2}{2\delta^2 \overline{\gamma}_{RD}^2}}}{\sqrt{2\pi\delta^2 \overline{\gamma}_{RD}^2}}, \tag{20}$$

where $s = N\pi/4$ and $\delta^2 = N\left(1 - \pi^2/16\right)$.

Then, we utilize several mathematic steps, the CDF of γ_{RD} is given by

$$F_{\gamma_{RD}}(x) = \frac{1}{\sqrt{2\pi\delta^2 \overline{\gamma}_{RD}^2}} \left[\Phi(A,B,C,x) - \Phi(A,B,C,0)\right], \tag{21}$$

where

$$\begin{aligned} &\Phi(A,B,C,x) \\ &= \frac{1}{2}\sqrt{\pi/A} \exp\left(\frac{B^2 - AC}{A}\right) erf\left(\sqrt{A}x + B/\sqrt{A}\right), \end{aligned} \tag{22}$$

where $A = \frac{1}{2\delta^2 \overline{\gamma}_{RD}^2}$, $B = \frac{-s}{2\delta^2 \overline{\gamma}_{RD}}$ and $C = \frac{s^2}{2\delta^2}$, and $erf(x)$ denotes the error function defined in [59].

By utilizing [59], we can derive

$$erf(x) = \frac{2}{\sqrt{\pi}} \sum_{k=1}^{\infty} \frac{(-1)^{k+1} x^{2k-1}}{(2k-1)(k-1)!}. \tag{23}$$

With the help of [17], the PDF for γ_{RE} is obtained as

$$\begin{aligned} &f_{\gamma_{RE}}(x) \\ &= \sum_{q=1}^{\rho(\mathrm{A}_{RE})} \sum_{j=1}^{\tau_q(\mathrm{A}_{RE})} \chi_{q,j}(\mathrm{A}_{RE}) \frac{\mu_{\langle q \rangle}^{-j}}{(j-1)!} x^{j-1} e^{-x/\mu_{\langle q \rangle}}, \end{aligned} \tag{24}$$

where $\mathrm{A}_{RE} = \mathrm{diag}(\mu_1, \mu_1, \ldots, \mu_M)$, $\rho(\mathrm{A}_{RE})$ denotes the number of distinct diagonal factors of A_{RE}, $\mu_{\langle \rho(\mathrm{A}_{RE}) \rangle} < \ldots < \mu_{\langle 2 \rangle} < \mu_{\langle 1 \rangle}$ represent the descending order of $\mu_{\langle q \rangle}$, $\tau_q(\mathrm{A}_{RE})$ represents the multiplicity of $\mu_{\langle q \rangle}$, besides $\chi_{q,j}(\mathrm{A}_{RE})$ represents the (q,j)-th characteristic factor of A_{RE} [17].

C. SOP

By utilizing [52], the SOP of this paper could be written as

$$\Pr(C_S \leq C_0) = \Pr(C_B - C_E \leq C_0), \tag{25}$$

where $C_E = \log_2(1 + \gamma_E)$, $C_B = \log_2(1 + \gamma_B)$ and $C_0 = \log_2(1 + \gamma_0)$ with γ_0 being the target secrecy threshold. Besides, $\gamma_B = \gamma_F = \min(\gamma_R, \gamma_D)$ and $\gamma_E = \gamma_{SE} + \gamma_{RE}$.

Theorem 1. *The final expression for the SOP of the regarded systems is given as* (26)*. It is shown in the beginning of 6-th page. Through* (26)*,* $\mathrm{K}(a,b,c,d,e,f,\gamma_0)$ *is written as* (27)*, which could be found at the beginning of 6-th page.* H *could be shown as*

$$\begin{aligned} H = &\frac{1}{\sqrt{2\pi A \delta^2 \overline{\gamma}_{RD}^2}} \exp\left(\frac{B^2 - AC}{A}\right) \\ &\times \sum_{k=1}^{\infty} \frac{(-1)^{k+1} B^{2k-1}}{A^{k-1/2} (k-1)! (2k-1)}. \end{aligned} \tag{28}$$

Proof: *See Appendix A.* ■

D. Asymptotic SOP

In this subsection, the asymptotic SOP would be provided. With the average SNR becoming infinite, i.e., $\overline{\gamma}_{SR} \to \infty$ and $\overline{\gamma}_{RD} \to \infty$, (18) and (21) can be re-written, respectively, by

$$F_{\gamma_{SR}}(x) = \frac{\alpha_{SR} x}{\overline{\gamma}_{SR}} + o(x), \tag{29}$$

and

$$F_{\gamma_{RD}}(x) = \frac{x e^{-\frac{s^2}{2\delta^2}}}{\overline{\gamma}_{RD} \sqrt{2\pi\delta^2}} + o(x), \tag{30}$$

where $o(x)$ denotes the higher order of x.

Theorem 2. *The asymptotic expression for SOP in high SNR scenario is written as*

$$\begin{aligned} \Pr(C_S \leq C_0) = &\sum_{\xi_1=0}^{m_{SE}-1} \cdots \sum_{\xi_M=0}^{m_{SE}-1} \sum_{q=1}^{\rho(\mathrm{A}_{RE})} \sum_{j=1}^{\tau_q(\mathrm{A}_{RE})} \frac{\alpha_{SR} \Xi(M)}{\overline{\gamma}_{SR} \mu_{\langle q \rangle}^j} \\ &\times \frac{\chi_{q,j}(\mathrm{A}_{RE})}{(j-1)!} \mathrm{K}\left(1, -, \Lambda_{SE} - 1, \Delta_{SE}, j-1, 1/\mu_{\langle q \rangle}, \gamma_0\right) \end{aligned}$$

$$\begin{aligned}
&\Pr\left(C_S \le C_0\right) = 1 - \sum_{k_1=0}^{m_{SR}-1}\sum_{t=0}^{k_1}\sum_{\xi_1=0}^{m_{SE}-1}\cdots\sum_{\xi_M=0}^{m_{SE}-1}\sum_{q=1}^{\rho(\mathrm{A}_{RE})}\sum_{j=1}^{\tau_q(\mathrm{A}_{RE})}\frac{\alpha_{SR}(1-m_{SR})_{k_1}(-\delta_{SR})^{k_1}\Xi(M)\chi_{q,j}(\mathrm{A}_{RE})}{\mu_{\langle q\rangle}^{j}(j-1)!k_1!t!\bar{\gamma}_{SR}^{k_1+1}\Delta_{SR}^{k_1-t+1}}\\
&\times \mathrm{K}\left(t,\Delta_{SR},\Lambda_{SE}-1,\Delta_{SE},j-1,1/\mu_{\langle q\rangle},\gamma_0\right) + \sum_{k_1=0}^{m_{SR}-1}\sum_{t=0}^{k_1}\sum_{\xi_1=0}^{m_{SE}-1}\cdots\sum_{\xi_M=0}^{m_{SE}-1}\sum_{q=1}^{\rho(\mathrm{A}_{RE})}\sum_{j=1}^{\tau_q(\mathrm{A}_{RE})}\frac{\Xi(M)\chi_{q,j}(\mathrm{A}_{RE})}{(j-1)!\mu_{\langle q\rangle}^{j}}\\
&\times\frac{\alpha_{SR}(1-m_{SR})_{k_1}(-\delta_{SR})^{k_1}}{k_1!t!\bar{\gamma}_{SR}^{k_1+1}\Delta_{SR}^{k_1-t+1}\sqrt{2\pi a\delta^2\bar{\gamma}_{RD}^2}}\exp\left(\frac{B^2-AC}{A}\right)\sum_{k=1}^{\infty}\sum_{p}^{2k-1}\binom{2k-1}{p}\frac{B^{2k-1-p}(-1)^{k+1}}{A^{k-1/2-p}(2k-1)(k-1)!}\\
&\times \mathrm{K}\left(t+p,\Delta_{SR},\Lambda_{SE}-1,\Delta_{SE},j-1,1/\mu_{\langle q\rangle},\gamma_0\right) - \sum_{k_1=0}^{m_{SR}-1}\sum_{t=0}^{k_1}\frac{\alpha_{SR}(1-m_{SR})_{k_1}(-\delta_{SR})^{k_1}}{k_1!t!\bar{\gamma}_{SR}^{k_1+1}\Delta_{SR}^{k_1-t+1}}\\
&\times\sum_{\xi_1=0}^{m_{SE}-1}\cdots\sum_{\xi_M=0}^{m_{SE}-1}\sum_{q=1}^{\rho(\mathrm{A}_{RE})}\sum_{j=1}^{\tau_q(\mathrm{A}_{RE})}\frac{\Xi(M)\chi_{q,j}(\mathrm{A}_{RE})H}{(j-1)!\mu_{\langle q\rangle}^{j}}\mathrm{K}\left(t,\Delta_{SR},\Lambda_{SE}-1,\Delta_{SE},j-1,1/\mu_{\langle q\rangle},\gamma_0\right). \qquad (26)
\end{aligned}$$

$$\begin{aligned}
&\mathrm{K}(a,b,c,d,e,f,\gamma_0) = \int_0^\infty\int_0^\infty z^a e^{-bz}\,|[(1+\gamma_0)x+(1+\gamma_0)y+\gamma_0]\,x^c e^{-dx}y^e e^{-fy}dxdy\\
&=\exp(-b\gamma_0)\sum_{l=0}^{a}\sum_{v=0}^{a-l}\binom{a}{l}\binom{a-l}{v}\gamma_0^{a-l-v}(1+\gamma_0)^{l+v}(l+c)!(v+e)![b(1+\gamma_0)+d]^{-l-c-1}[b(1+\gamma_0)+f]^{-v-e-1}. \qquad (27)
\end{aligned}$$

$$\begin{aligned}
&+\sum_{\xi_1=0}^{m_{SE}-1}\cdots\sum_{\xi_M=0}^{m_{SE}-1}\sum_{q=1}^{\rho(\mathrm{A}_{RE})}\sum_{j=1}^{\tau_q(\mathrm{A}_{RE})}\frac{\Xi(M)e^{-\frac{s^2}{2\delta^2}}\chi_{q,j}(\mathrm{A}_{RE})}{(j-1)!\mu_{\langle q\rangle}^{j}\sqrt{2\pi a\delta^2\bar{\gamma}_{RD}^2}}\\
&\times\mathrm{K}\left(1,-,\Lambda_{SE}-1,\Delta_{SE},j-1,1/\mu_{\langle q\rangle},\gamma_0\right). \qquad (31)
\end{aligned}$$

Proof: By replacing (18) *(*$V = SR$*) and* (21) *with* (29) *and* (30)*, respectively. Then by utilizing the similar way through Appendix A, the* **Theorem 2** *can be proved.* ■

From (31), when $\bar{\gamma}_{SR} = \bar{\gamma}_{RD} = \bar{\gamma}$, we can derive the SDO and the SCG by some calculating steps. The SDO and SCG are, respectively, shown as

$$G_{SDO} = 1, \qquad (32)$$

and

$$\begin{aligned}
&G_{SCG} = \sum_{\xi_1=0}^{m_{SE}-1}\cdots\sum_{\xi_M=0}^{m_{SE}-1}\sum_{q=1}^{\rho(\mathrm{A}_{RE})}\sum_{j=1}^{\tau_q(\mathrm{A}_{RE})}\frac{\alpha_{SR}\Xi(M)}{\mu_{\langle q\rangle}^{j}}\\
&\times\frac{\chi_{q,j}(\mathrm{A}_{RE})}{(j-1)!}\mathrm{K}\left(1,-,\Lambda_{SE}-1,\Delta_{SE},j-1,1/\mu_{\langle q\rangle},\gamma_0\right)\\
&+\sum_{\xi_1=0}^{m_{SE}-1}\cdots\sum_{\xi_M=0}^{m_{SE}-1}\sum_{q=1}^{\rho(\mathrm{A}_{RE})}\sum_{j=1}^{\tau_q(\mathrm{A}_{RE})}\frac{\Xi(M)e^{-\frac{s^2}{2\delta^2}}\chi_{q,j}(\mathrm{A}_{RE})}{(j-1)!\mu_{\langle q\rangle}^{j}\sqrt{2\pi a\delta^2}}\\
&\times\mathrm{K}\left(1,-,\Lambda_{SE}-1,\Delta_{SE},j-1,1/\mu_{\langle q\rangle},\gamma_0\right). \qquad (33)
\end{aligned}$$

IV. Numerical Results

Through the following section, several representative MC investigations are given to show the rightness of the theoretical ones. The channel and system parameters are provided into Table II with $Q \in \{V, SE\}$ [19] and Table III [51], [52], respectively. By using [43] and [38], $A = 1$, $L_{RV_i} = L_{V_iD} = L = 20$, $\bar{\gamma}_{SR} = \bar{\gamma}_{RD} = \bar{\gamma}$ and $\bar{\gamma}_{SE} = \bar{\gamma}_{RE} = \bar{\gamma}_E$ are regarded. Besides, by using the infinite series function, when $N = 2$, 10 terms is enough; when $N = 10$, 30 terms is also enough. In addition, the software used is Matlab.

TABLE II
CHANNEL PARAMETERS

Shadowing	m_Q	b_Q	Ω_Q
Infrequent light shadowing (ILS)	10	0.158	1.29
Frequent heavy shadowing (FHS)	1	0.063	0.0007
Average shadowing (AS)	5	0.251	0.279

TABLE III
SYSTEM PARAMETERS

Parameters	Value
Satellite Orbit	GEO
Noise Temperature	300°K
3dB angle	$\vartheta_{3\mathrm{dB}} = 0.8°$
Frequency band	f=2GHz
link bandwidth	$W = 15$MHz
Maximal Beam Gain	$G_{max} = 48dB$

Fig. 2 illustrates the SOP versus $\bar{\gamma}$ for different γ_0 and different shadowing with $\bar{\gamma}_E$=1 dB, N=2 and M=1. In Fig. 2, it could be found that the MC ones are very similar to the theoretical ones, which prove the accuracy and correctness of the theoretical analysis. Moreover, the approximate results are same with the MC ones and theoretical ones in high SNR regime. In addition, it could also be known that if channel undergoes heavy fading, the SOP would larger for the signal is enhanced by the channel fading. Finally, we derive that when the threshold goes smaller, the SOP will be lower, too.

Fig. 3 depicts the SOP versus $\bar{\gamma}$ for several M and several $\bar{\gamma}_E$ with γ_0=1 dB and N=2 under FHS scenario. Derived from

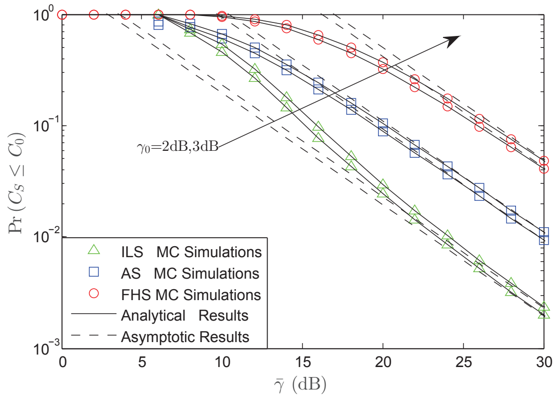

Fig. 2. SOP versus $\bar{\gamma}$ for several γ_0 and different shadowing with $\bar{\gamma}_E$=1 dB, N=2 and M=1.

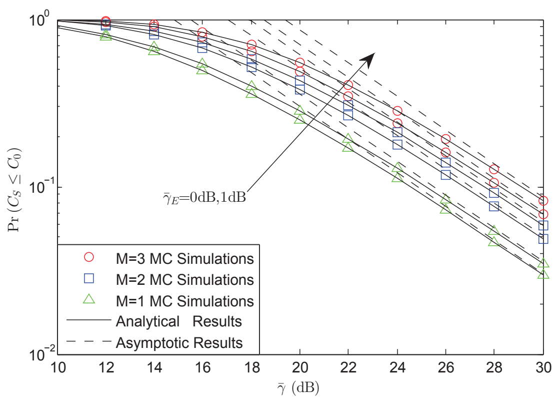

Fig. 3. SOP versus $\bar{\gamma}$ for several M and several $\bar{\gamma}_E$ with γ_0=1 dB and $N=2$ under FHS scenario.

Fig. 3, with M becoming larger, the SOP would be larger as the result that more Eves participate in overhearing the legitimate user's information. Moreover, we can get that when the power of eavesdroppers becomes smaller, the SOP will be lower resulting from that the Eves have much power to steal the information.

Fig. 4 represents the SOP versus $\bar{\gamma}$ for some $\bar{\gamma}_E$ and several γ_0 with N=2 and M=1 under FHS case. Obtained from Fig. 4, it can be obtained that when the threshold of the system gets

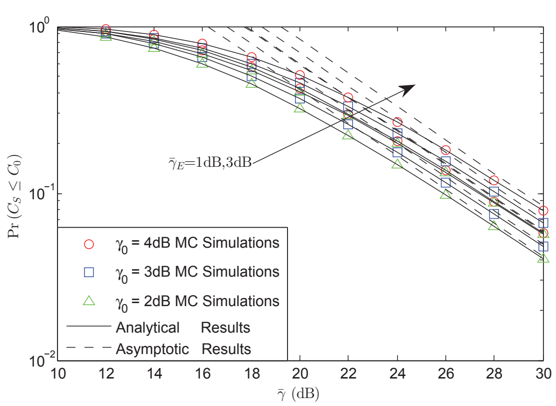

Fig. 4. SOP versus $\bar{\gamma}$ for several $\bar{\gamma}_E$ and different γ_0 with N=2 and M=1 under FHS scenario.

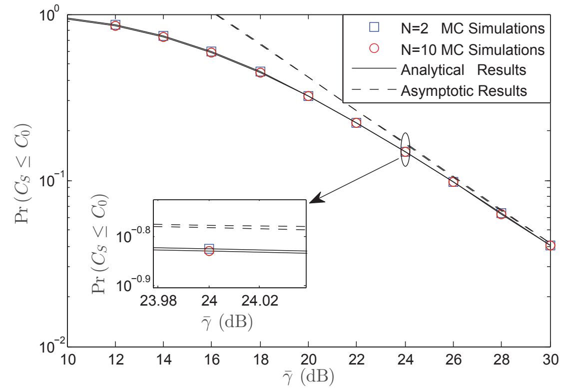

Fig. 5. SOP versus $\bar{\gamma}$ for several N with γ_0=2 dB, $\bar{\gamma}_E$=1 dB and M=1 under FHS scenario.

smaller the SOP will be lower, too. The similar results with the Fig. 2 and Fig. 3, the MC simulations are still similar to the analytical ones. The approximate ones are equivalent with theoretical investigations at high SNRs.

Fig. 5 examines SOP versus $\bar{\gamma}$ for several N with γ_0=2 dB, $\bar{\gamma}_E$=1 dB and M=1 under FHS case. Upon Fig. 5, it could be derived that when N becomes larger, a lower SOP would appear, however, we find that the impact of N is less serious than that of the other system parameters which results from that the channel quality of $S \to R$ link plays a major role in the transmission quality.

V. Conclusions

Through the whole paper, the secrecy issues for the RIS-based ISUAVRNs was investigated, especially, the final expressions were also derived. Through the obtained theoretical results, the impacts for the main system and channel parameters were further gotten. From the derived results, we could see that a light channel shadowing, more N and lower M could lead to a better secrecy performance.

Appendix A
Proof of Theorem 1

Reconsidering (25), it can be obtained that

$$\begin{aligned}
&\Pr(C_S \le C_0) = \Pr(C_B - C_E \le C_0) \\
&= \Pr\left[\log_2(1+\gamma_B) - \log_2(1+\gamma_E) \le \log_2(1+\gamma_0)\right] \\
&= \Pr\left[\gamma_B \le \gamma_0 + \gamma_E(1+\gamma_0)\right] \\
&= \int_0^\infty \int_0^{\gamma_0+y(1+\gamma_0)} f_{\gamma_B}(x) f_{\gamma_E}(y)\, dx dy \\
&= \int_0^\infty F_{\gamma_B}(\gamma_0 + y(1+\gamma_0)) f_{\gamma_E}(y)\, dx dy. \qquad (34)
\end{aligned}$$

From (34), it could be found the major part is to obtain the CDF of γ_B. By utilizing (12) and (25), the CDF for γ_B is re-written as

$$\begin{aligned}
F_{\gamma_B}(x) &= \Pr(\gamma_B \le x) = \Pr\left[\min(\gamma_{SR}, \gamma_{RD}) \le x\right] \\
&= \Pr(\gamma_{SR} \le x) + \Pr(\gamma_{RD} \le x) \\
&\quad - \Pr(\gamma_{SR} \le x)\Pr(\gamma_{RD} \le x). \qquad (35)
\end{aligned}$$

Then, by substituting (18) ($V=SR$) and (21) into (35) and after some calculations, (35) can be re-given as

$$F_{\gamma_B}(x) = 1-\Theta_1 - H\Theta_1 + \Theta_2, \tag{36}$$

where

$$\Theta_1 = \sum_{k_1=0}^{m_{SR}-1}\sum_{t=0}^{k_1} \frac{\alpha_{SR}(1-m_{SR})_{k_1}(-\delta_{SR})^{k_1}x^t}{k_1!t!\bar{\gamma}_{SR}^{k_1+1}\Delta_{SR}^{k_1-t+1}\exp(\Delta_{SR}x)}$$

$$\Theta_2 = \sum_{k_1=0}^{m_{SR}-1}\sum_{t=0}^{k_1}\sum_{k=1}^{\infty}\sum_{p}^{2k-1} \frac{\binom{2k-1}{p}B^{2k-1-p}(-1)^{k+1}x^{t+p}}{A^{k-1/2-p}(2k-1)(k-1)!}$$
$$\times \frac{\alpha_{SR}(1-m_{SR})_{k_1}(-\delta_{SR})^{k_1}\exp\left(\frac{B^2-AC}{A}\right)}{\sqrt{2\pi a\delta^2\bar{\gamma}_{RD}^2}k_1!t!\bar{\gamma}_{SR}^{k_1+1}\Delta_{SR}^{k_1-t+1}\exp(\Delta_{SR}x)}.$$

Then, by inserting (36) into (34), (34) is re-written as

$$\begin{aligned}
&\Pr(C_S \le C_0)\\
&= 1-\int_0^\infty\int_0^\infty (\Theta_1 + H\Theta_1 - \Theta_2)\,|[\gamma_0 + y(1+\gamma_0)]\\
&\times f_{\gamma_{SE}}(y)f_{\gamma_{RE}}(z)\,dydz\\
&= 1 - J_1 - HJ_1 + J_2,
\end{aligned} \tag{37}$$

where

$$J_1 = \int_0^\infty\int_0^\infty \Theta_1\,|[\gamma_0 + (y+z)(1+\gamma_0)]\,f_{\gamma_{SE}}(y)f_{\gamma_{RE}}(z)\,dydz$$
$$J_2 = \int_0^\infty\int_0^\infty \Theta_2\,|[\gamma_0 + (y+z)(1+\gamma_0)]\,f_{\gamma_{SE}}(y)f_{\gamma_{RE}}(z)\,dydz,$$

and

$$f(x)\,|b = f(b). \tag{38}$$

Next, by taking J_1 as an example, by inserting (19) and (24) into J_1, after some mathematical steps, J_1 could be written as

$$\begin{aligned}
&J_1\\
&= \int_0^\infty\int_0^\infty \Theta_1\,|\gamma_0 + (y+z)(1+\gamma_0)\,f_{\gamma_{SE}}(y)f_{\gamma_{RE}}(z)\,dydz\\
&= \sum_{\xi_1=0}^{m_{SE}-1}\cdots\sum_{\xi_M=0}^{m_{SE}-1}\sum_{q=1}^{\rho(\mathrm{A}_{RE})}\sum_{j=1}^{\tau_q(\mathrm{A}_{RE})}\sum_{k_1=0}^{m_{SR}-1}\sum_{t=0}^{k_1}\frac{\alpha_{SR}\Xi(M)}{(j-1)!}\\
&\times \frac{\chi_{q,j}(\mathrm{A}_{RE})(1-m_{SR})_{k_1}}{k_1!t!\bar{\gamma}_{SR}^{k_1+1}\Delta_{SR}^{k_1-t+1}\mu_{\langle q\rangle}^j(-\delta_{SR})^{-k_1}}\\
&\times K\left(t,\Delta_{SR},\Lambda_{SE}-1,\Delta_{SE},j-1,\frac{1}{\mu_{\langle q\rangle}},\gamma_0\right),
\end{aligned} \tag{39}$$

where

$$\begin{aligned}
&K\left(t,\Delta_{SR},\Lambda_{SE}-1,\Delta_{SE},j-1,\frac{1}{\mu_{\langle q\rangle}},\gamma_0\right)\\
&= \int_0^\infty\int_0^\infty [\gamma_0 + (y+z)(1+\gamma_0)]^t \frac{y^{\Lambda_{SE}-1}}{e^{\Delta_{SR}[\gamma_0+(y+z)(1+\gamma_0)]}}\\
&\times \exp(-\Delta_{SE}y)\,z^{j-1}\exp\left(-z/\mu_{\langle q\rangle}\right)dydz\\
&= \sum_{v=0}^{t}\sum_{q=0}^{t-v}\binom{t}{v}\binom{t-v}{q}\frac{(1+\gamma_0)^{v+q}}{\gamma_0^{q+v-t}}\mathrm{H}_1\mathrm{H}_2.
\end{aligned}$$

In (39), by utilizing [59], H_1 and H_2 can be written as

$$\mathrm{H}_1 = \frac{(v+\Lambda_{SE}-1)!}{[\Delta_{SE}+(1+\gamma_0)\Delta_{SR}]^{-v-\Lambda_{SE}}}, \tag{40}$$

$$\mathrm{H}_2 = \frac{(q+j-1)!}{\left[1/\mu_{\langle q\rangle}+(1+\gamma_0)\Delta_{SR}\right]^{-v-\Lambda_{SE}}}. \tag{41}$$

Then, by taking (40) and (41) into (39), J_1 along with $\mathrm{K}(a,b,c,d,e,f,\gamma_0)$ can be obtained.

Then, with the similar method, J_2 can be derived as

$$\begin{aligned}
&J_2\\
&= \sum_{k_1=0}^{m_{SR}-1}\sum_{t=0}^{k_1}\sum_{\xi_1=0}^{m_{SE}-1}\cdots\sum_{\xi_M=0}^{m_{SE}-1}\sum_{q=1}^{\rho(\mathrm{A}_{RE})}\sum_{j=1}^{\tau_q(\mathrm{A}_{RE})}\frac{\chi_{q,j}(\mathrm{A}_{RE})}{(j-1)!}\\
&\times \frac{\Xi(M)}{\mu_{\langle q\rangle}^j}\mathrm{K}\left(t+p,\Delta_{SR},\Lambda_{SE}-1,\Delta_{SE},j-1,1/\mu_{\langle q\rangle},\gamma_0\right)\\
&\times \frac{\alpha_{SR}(1-m_{SR})_{k_1}(-\delta_{SR})^{k_1}}{k_1!t!\bar{\gamma}_{SR}^{k_1+1}\Delta_{SR}^{k_1-t+1}\sqrt{2\pi a\delta^2\bar{\gamma}_{RD}^2}}\exp\left(\frac{B^2-AC}{A}\right)\\
&\times \sum_{k=1}^{\infty}\sum_{p}^{2k-1}\binom{2k-1}{p}\frac{B^{2k-1-p}(-1)^{k+1}}{A^{k-1/2-p}(2k-1)(k-1)!}.
\end{aligned} \tag{42}$$

Finally, by inserting J_1 and J_2 into (37), (26) can be derived, the end.

References

[1] G. Ma, S. Dang, M.-S. Alouini, and B. Shihada, "Smart buildings enabled by 6G communications," *IEEE Internet of Things Mag.*, vol. 5, no. 2, pp. 181-186, Jun. 2022.

[2] G. Pan, J. Ye, J. An and S. Alouini, "Latency versus reliability in LEO mega-constellations: Terrestrial, Aerial, or space relay," *IEEE Trans. Mobile Computing*, early access, pp. 1-1, Apr. 2022.

[3] X. Li, J. Li, Y. Liu, Z. Ding, and A. Nallanathan, "Residual transceiver hardware impairments on cooperative NOMA networks," *IEEE Trans. Wireless Commun.*, vol. 19, no. 1, pp. 680-695, Jan. 2020.

[4] K. An, T. Liang, G. Zheng, X. Yan, Y. Li, and S. Chatzinotas, "Performance limits of cognitive-uplink FSS and terrestrial FS for Ka-band," *IEEE Trans. Aeros. Elec. Syst.*, vol. 55, no. 5, pp. 2604-2611, Oct. 2019.

[5] L. Xu, et al., "Mobile collaborative secrecy performance prediction for artificial IoT networks," *IEEE Trans. Industrial Informatics*, vol. 18, no. 8, pp. 5403-5411, Aug. 2022.

[6] K. Guo, M. Lin, B. Zhang, W.-P. Zhu, J.-B. Wang, and T. A. Tsiftsis, "On the performance of LMS communication with hardware impairments and interference," *IEEE Trans. Commun.*, vol. 67, no. 2, pp. 1490-1505, Feb. 2019.

[7] Z. N. Chen, X. Qing, X. Tang, W. E. I. Liu, and R. Xu, "Phased array metantennas for satellite communications," *IEEE Commun. Mag.*, vol. 60, no. 1, pp. 46-50, Jan. 2022.

[8] C. Liu, W. Feng, Y. Chen, C.-X. Wang, and N. Ge, "Cell-free satellite-UAV networks for 6G wide-area internet of things," *IEEE J. Sel. Area Commun.*, vol. 39, no. 4, pp. 1116-1131, Apr. 2021.

[9] Y. Sun and M. Peng, "Edge intelligence assisted resource management for satellite communication," *China Commun.*, vol. 19, no. 8, pp. 31-40, Aug. 2022.

[10] D. Peng, D. He, Y. Li, and Z. Wang, "Integrating terrestrial and satellite multibeam systems toward 6G: Techniques and challenges for interference mitigation," *IEEE Wireless Commun.*, vol. 29, no. 1, pp. 24-31, Feb. 2022.

[11] X. Hou, J. Wang, Z. Fang, Y. Ren, K. C. Chen, and L. Hanzo, "Edge intelligence for mission-critical 6G services in space-air-ground integrated networks," *IEEE Network*, vol. 36, no. 2, pp. 181-189, Apr. 2022.

[12] I. C. Msadaa, S. Zairi, and A. Dhraief, "Non-terrestrial networks in a nutshell," *IEEE Internet of Things J.*, vol. 5, no. 2, pp. 168-174, Jun. 2022.

[13] G. Giambene, S. Kota, and P. Pillai, "Satellite-5G integration: A network perspective," *IEEE Network*, vol. 32, no. 5, pp. 25-31, Oct. 2018.

[14] H. Guo, J. Li, J. Liu, M. Tian, and N. Kato, "A survey on space-air-ground-sea integrated network security in 6G," *IEEE Commun. Surveys Tut.*, vol. 24, no. 1, pp. 53-87, Firstquarter, 2022.

[15] B. Mao, F. Tang, Y. Kawamoto, and N. Kato, "Optimizing computation offloading in satelllite-UAV-served 6G IoT: A deep learninng approach," *IEEE Network*, vol. 35, no. 4, pp. 102-108, Aug. 2021.

[16] M. A. Rahman and M. Hossain, "Design of a secure internet of artificially intelligent things in the 6G Era," *IEEE Internet of Things Mag.*, vol. 5, no. 2, pp. 49-54, Jun. 2022.

[17] K. Guo, K. An, B. Zhang, Y. Huang, D. Guo, G. Zheng, and S. Chatzinotas, "On the performance of the uplink satellite multi-terrestrial relay networks with hardware impairments and interference," *IEEE Syst. J.*, vol. 13, no. 3, pp. 2297-2308, Sep. 2019.

[18] K. Guo, M. Lin, B. Zhang, J.-B. Wang, Y. Wu, W.-P. Zhu, and J. Cheng, "Performance analysis of hybrid satellite-terrestrial cooperative networks with relay selection," *IEEE Trans. Vehi. Technol.*, vol. 69, no. 8, pp. 9053-9067, Aug. 2020.

[19] K. Guo, K. An, F. Zhou, T. A. Tsiftsis, G. Zheng, and S. Chatzinotas, "On the secrecy performance of NOMA-based integrated satellite multiple-terrestrial relay networks with hardware impairments," *IEEE Trans. Vehi. Technol.*, vol. 70, no. 4, pp. 3661-3676, Apr. 2021.

[20] P. K. Sharma, P. K. Upadhyay, D. B. da Costa, P. S. Bithas, and A. G. Kanatas, "Performance analysis of overlay spectrum sharing in hybrid satellite-terrestrial systems with secondary network selection," *IEEE Trans. Wireless Commun.*, vol. 16, no. 10, pp. 6586-6601, Oct. 2017.

[21] P. K. Upadhyay and P. K. Sharma, "Max-max user-relay selection scheme in multiuser and multirelay hybrid satellite-terrestrial relay systems," *IEEE Commun. Lett.*, vol. 20, no. 2, pp. 268-271, Jan. 2016.

[22] J. Wang, C. Jiang, Z. Wei, C. Pan, H. Zhang, and Y. Ren, "Joint UAV hovering altitude and power control for space-air-ground IoT networks," *IEEE Internet of Things J.*, vol. 6, no. 2, pp. 1741-1753, Apr. 2019.

[23] N. Kato, Z. M. Fadlullah, F. Tang, and B. Mao, "Optimizing space-air-ground integrated networks by artificial intelligence," *IEEE Wireless Commun.*, vol. 26, no. 4, pp. 140-147, Aug. 2019.

[24] M. Lin, Q. Huang, T. de. Cola, J.-B. Wang, J. Wang, M. Guizani, and J.-Y. Wang, "Integrated 5G-satellite networks: A perspective on physical layer relibility and security," *IEEE Wireless Commun.*, vol. 27, no. 6, pp. 152-159, Dec. 2020.

[25] X. Li and W. Shi, "Hybrid satellite-UAV-terrestrial maritime networks: Network selection for users on a vessel optimized with transmit power and UAV position," *China Commun.*, vol. 19, no. 9, pp. 37-46, Sep. 2022.

[26] C. Han, A. Liu, K. An, H. Wang, and G. Zheng, "Satellite-assisted UAV trajectory control in hostile jamming environments," *IEEE Trans. Vehi. Technol.*, vol. 71, no. 4, pp. 3760-3775, Apr. 2022.

[27] Z. Yin, N. Cheng, T. H. Luan, and P. Wang, "Physical layer security in cybertwin-enabled integrated satellite-terrestrial vehicle networks," *IEEE Trans. Vehi. Technol.*, vol. 71, no. 5, pp. 4561-4572, May 2022.

[28] F. Pervez, L. Zhao, and C. yang, "Joint user association, Power optimization and trajectory control in an integrated satellite-aerial-terrestrial network," *IEEE Trans. Wireless Commun.*, vol. 21, no. 5, pp. 3279-3290, May 2022.

[29] C. Huang, A. Zappone, G. C. Alexandropoulos, M. Debbah, and C. Yuen, "Reconfigurable intelligent surfaces for energy efficiency in wireless communication," *IEEE Trans. Wireless Commun.*, vol. 18, no. 8, pp. 4157-4170, Aug. 2019.

[30] B. Di, H. Zhang, L. Song, Y. Li, Z. Han, and H. V. Poor, "Hybrid beamforming for reconfigurable intelligent surface based multi-user communications: Achievable rates with limited discrete phase shifts," *IEEE J. Sel. Areas Commun.*, vol. 38, no. 8, pp. 1809-1822, Aug. 2020.

[31] C. Huang, R. Mo. and C. Yuen, "Reconfigurable intelligent surface assisted multiuser MISO systems exploiting deep reinforcement learning," *IEEE J. Sel. Areas Commun.*, vol. 38, no. 8, pp. 1839-1850, Aug. 2020.

[32] Y. Su, X. Pang, S. Chen, X. Jiang, N. Zhao, and F. R. Yu, "Spectrum and energy efficiency optimization in IRS-assisted UAV networks," *IEEE Trans. Commun.*, vol. 70, no. 10, pp. 6489-6502, Oct. 2022.

[33] Z. Lin, et al., "Refracting RIS aided hybrid satellite-terrestrial relay networks: Joint beamforming design and optimization," *IEEE Trans. Aeros. Elect. Syst.*, vol. 58, no. 4, 2022.

[34] S. Li, B. Duo, X. Yuan, Y.-C. Liang, and M. D. Renzo, "Reconfigurable intelligent surface assisted UAV communication: Joint trajectory design and passive beamforming," *IEEE Wirless Commun. Lett.*, vol. 9, no. 5, pp. 716-720, May 2020.

[35] E. Basar, "Reconfigurable intelligent surface-based index modulation: A new beyond MIMO paradigm for 6G," *IEEE Trans. Commun.*, vol. 68, no. 5, pp. 3187-3196, May 2020.

[36] G. Zhou, C. Pan, H. Ren, K. Wang, and A. Nallanathan, "A framework of robust transmission design for IRS-aided MISO communications with imperfect cascaded channels," *IEEE Trans. Sig. Processing*, vol. 68, pp. 5092-5106, Aug. 2020.

[37] X. Pang, M. Sheng, N. Zhao, J, Tang, D. Niyato, and K. K. Wong, "When UAV meets IRS: Expanding air-ground networks via passive reflection," *IEEE Wireless Commun.*, vol. 28, no. 5, pp. 164-170, Oct. 2021.

[38] L. Yang, F. Meng, J. Zhang, M. O. Hasna, and M. D. Renzo, "On the performance of RIS-assisted dual-hop UAV communication systems," *IEEE Trans. Vehi. Technol.*, vol. 69, no. 9, pp. 10385-10390, Sep. 2020.

[39] N. Agrawal, A. Bansal, K. Singh, and C.-P, Li, "Performance evaluation of RIS-assisted UAV-enabled vehicular communication system with multiple non-identical interferes," *IEEE Trans. Intelligent Transportation Syst.*, vol. 23, no. 7, pp. 9883-9894, Jul. 2022.

[40] H. Mei, K. Yang, Q. Liu, and K. Wang, "3D-trajectory and phase-shift design for RIS-assisted UAV systems using deep reinforcement learning," *IEEE Trans. Vehi. Technol.*, vol. 71, no. 3, pp. 3020-3029, Mar. 2022.

[41] A. Khalili, et al., "Resource management for transmit power minimization in UAV-assited RIS hetnets supported by dual connectivity," *IEEE Trans. Wireless Commun.*, vol. 21, no. 3, pp. 1806-1822, Mar. 2022.

[42] T. V. Nguyen, et al., "On the design of RIS-UAV relay-assisted hybrid FSO/RF satellite-aerial-ground integrated network," *IEEE Trans. Aero. Electronic Syst.*, early access, pp. 1-15, Jul. 2022.

[43] K. Guo and K. An, "On the performance of RIS-assisted integrated satellite-UAV-terrestrial networks with hardware impairemnts and interference," *IEEE Wireless Commun. Lett.*, vol. 11, no. 1, pp. 131-135, Jan. 2022.

[44] H. Liu, G. Li, X. Li, G. Huang, Y. Liu and Z. Ding, "Effective capacity analysis of STAR-RIS assisted NOMA networks," *IEEE Wireless Commun. Lett.*, vol. 11, no. 9, pp. 1930-1934, Sep. 2022.

[45] X. Li, Y. Zheng, M .Zeng, Y. Liu, O. A. Dobre, "Enhancing secrecy performance for STAR-RIS NOMA networks," *IEEE Trans. Vehi. Technol.*, early access, pp. 1-6, Oct. 2022.

[46] X. Li, M. Zhao, Y. Liu, L. Li, Z. Ding, and A. Nallanathan, "Secrecy analysis of ambient backscatter NOMA systems under I/Q imbalance," *IEEE Trans. Vehi. Technol.*, vol. 69, no. 10, pp. 12286-12290, Oct. 2020.

[47] X. Li, M. Zhao, M. Zeng, S. Mumtaz, V. G. Menon, Z. Ding, and O. A. Dobre, "Hardware impaired ambient backscatter NOMA systems: Reliability and security," *IEEE Trans. Commun.*, vol. 69, no. 4, pp. 2723-2736, Apr. 2021.

[48] K. An, M. Lin, J. Ouyang, and W.-P. Zhu, "Secure transmission in cognitive satellite terrestrial networks," *IEEE J. Sel. Areas Commun.*, vol. 34, no. 11, pp. 3025-3037, Nov. 2016.

[49] K. Guo, X. Li, M. Alazab, R. H. Jhaveri, and K. An, "Integrated satellite multiple two-way telay networks: Secrecy performance under multiple eves and vehicles with non-ideal hardware," *IEEE Trans. Intelligent Vehi.*, early access, pp. 1-12, Oct. 2022.

[50] B. Li, Z. Fei, C. Zhou, and Y. Zhang, "Physical layer security in space information networks: A survey," *IEEE Internet of Things J.*, vol. 7, no. 1, pp. 33-52, Jan. 2020.

[51] K. Guo, C. Dong, and K. An, "NOMA-based cognitive satellite terrestrial relay network: Secrecy performance under channel estimation errors and hardware impairments," *IEEE Internet of Things J.*, vol. 9. no. 18, pp. 17334-17347, Sep. 2022.

[52] K. Guo, K. An, B. Zhang, Y. Huang, X. Tang, G. Zheng, and T. A. Tsiftsis, "Physical layer security for multiuser satellite communication systems with threshold-based scheduling scheme," *IEEE Trans. Vehi. Technol.*, vol. 69, no. 5, pp. 5129-5141, May 2020.

[53] B. Li, Z. Fei, Z. Chu, F. Zhou, K. K. Wong, and P. Xiao, "Robust chance-constrained secure transmission for cognitive satellite-terrestrial networks," *IEEE Trans. Vehi. Technol.*, vol. 67, no. 5, pp. 4208-4219, May 2018.

[54] B. Li, Z. Fei, X. Xu, and Z. Chu, "Resource allocations for secure cognitive satellite-terrestrial networks," *IEEE Wireless Commun. Lett.*, vol. 7, no. 1, pp. 78-81, Feb. 2018.

[55] Z. Lin, M. Lin, B. Champagne, W.-P. Zhu, and N. A.-Dhahir, "Secrecy-energy efficient hybrid beamforming for satellite-terrestrial integrated networks," *IEEE Trans. Commun.*, vol. 69, no. 3, pp. 6345-6360, Sep. 2021.

[56] S. Li, B. Duo, M. D. Renzo, M. Tao, and X. Yan, "Robust secure UAV communication with the aid of reconfigurable intelligent surfaces," *IEEE Trans. Wireless Commun.*, vol. 20, no. 10, pp. 6401-6417, Oct. 2021.

[57] X. Guo, Y. Chen, and Y. Wang, "Learning-based robust and secure transmission for reconfigurable intelligent surface aided millimeter wave UAV communications," *IEEE Wireless Commun. Lett.*, vol. 10, no. 8, pp. 1795-1799, Aug. 2021.

[58] L. Wei, K. Wang, C. Pan, and M. Elkashlan, "Secrecy performance analysis of RIS-aided communication system with randomly flying eavesdroppers," *IEEE Wireless Commun. Lett.*, vol. 11, no. 10, pp. 2240-2244, Oct. 2022.

[59] I. S. Gradshteyn, I. M. Ryzhik, A. Jeffrey, et. al., "Table of integrals, series and products," *7thed.Amsterdam*, Boston: Elsevier, 2007.

[60] K. Guo, K. An, B. Zhang, Y. Huang, and G. Zheng, "Outage analysis of cognitive hybrid satellite-terrestrial networks with hardware impairments and multi-primary users," *IEEE Wireless Commun. Lett.*, vol. 7, no. 5, pp. 816-819. Oct. 2018.

Feng Zhou received the B.S. degrees and M.S. degrees from Southeast University, Nanjing, China, in 2004 and 2012 respectively. Since 2017, he has been an associate professor with the College of Information Engineering, Yancheng Institute of Technology, Yancheng, China. His research interests include cooperative communication, satellite communication, cognitive radio, physical layer security and UAV communication.

Xingwang Li (S'12-M'15-SM'20) received the M. Sc. and Ph. D. degrees from University of Electronic Science and Technology of China and Beijing University of Posts and Telecommunications in 2010 and 2015. From 2010 to 2012, he worked at Comba Telecom Ltd. In Guangzhou China, as an engineer. He spent one year from 2017 to 2018 as a visiting scholar at Queen's University Belfast, Belfast, UK. He is currently an Associated Professor with the School of Physics and Electronic Information Engineering, Henan Polytechnic University, Jiaozuo China. His research interests span wireless communication, intelligent transport system, artificial intelligence, Internet of things.

Dr. Li has served as many TPC members, such as the IEEE Globecom, IEEE ICC, IEEE WCNC, IEEE VTC, IEEE ICCC etc. He has also served as the Co-Chair for the IEEE/IET CSNDSP 2020 of the Green Communications and Networks Track. He also serves as an Editor on the Editorial Board for IEEE Transactions on Intelligent Transportation Systems, IEEE Transactions on Vehicular Technology, IEEE Systems Journal, Physical Communication. He was the Guest Editor for the special issue on Computational Intelligence and Advanced Learning for Next-Generation Industrial IoT of IEEE Transactions on Network Science and Engineering, "Recent Advances in Physical Layer Technologies for 5G-Enabled Internet of Things" of the Wireless Communications and Mobile Computing. He has served as many TPC members, such as IEEE ICC, GLOBECOM, WCNC, VTC, ICCC, etc. He is also the Co-Chair of IEEE/IET CSNDSP 2020 of the Green Communications and Networks track.

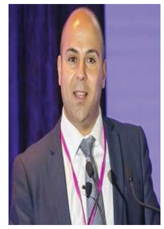

Mamoun Alazab is an Associate Professor at the College of Engineering, IT and Environment at Charles Darwin University, Australia. He is the recipient of the prestigious award: NT Young Tall Poppy (2021) of the year from the Australian Institute of Policy and Science (AIPS), and the Japan Society for the Promotion of Science (JSPS) fellowship through the Australian Academy of Science. He is a cyber security researcher and practitioner with industry and academic experience. He has more than 300 research papers (more than 90 % in Q1 and in the top 10 % of Journal articles, and more than 100 in IEEE/ACM Transactions) and 11 authored/edited books. He is a Senior Member of the IEEE, and the founding chair of the IEEE Northern Territory (NT) Subsection. He serves as the Associate Editor of IEEE Transactions on Computational Social Systems, IEEE Transactions on Network and Service Management (TNSM), IEEE Internet of Things Journal, ACM Digital Threats: Research and Practice, and Complex & Intelligent Systems.

Rutvij H. Jhaveri (Senior Member, IEEE) is an experienced educator and researcher working in the Department of Computer Science & Engineering, Pandit Deendayal Energy University, Gandhinagar, India. He conducted his Postdoctoral Research at Delta-NTU Corporate Lab for Cyber-Physical Systems, Nanyang Technological University, Singapore. He completed his PhD in Computer Engineerng in 2016. In 2017, he was awarded with prestigious Pedagogical Innovation Award by Gujarat Technological University. Currently, he is co-investigating a funded project from GUJCOST. He was ranked among top 2% s5ientists around the world in 2021. He has 2200+ Google Scholar citations with h-index 25. Apart from serving as an editor/ guest editor in various journals of repute, he also serves as a reviewer in several international journals and also as an advisory/TPC member in renowned international conferences. He authored 125+ articles including the IEEE/ACM Transactions and flagship IEEE/ACM conferences. Moreover, he has several national and international patents and, copyrights to his name. He also possesses memberships of various technical bodies such as ACM, CSI, ISTE, IDES and others. He is a member of the Advisory Board in Symbiosis Institute of Digital and Telecom Management, Manav Rachna Group and Sandip University since 2022. He is an editorial board member in several Hindawi and Springer journals. He also served as a committee member in "Smart Village Project" - Government of Gujarat, at the district level during the year 2017. His research interests are Cyber Security, IoT systems, SDN and Smart Healthcare.

Kefeng Guo (S'12-M'18) received his B.S. degree from Beijing Institute of Technology, Beijing, China, in 2012, the M.S. degree from PLA University of Science and Technology, Nanjing, China, in 2015 and the Ph.D. degree in Army Engineering University of PLA in 2018. He is a Lecturer in School of Space Information, Space Engineering University. He is also the associate professor in the College of Electronic and Information Engineering, Nanjing University of Aeronautics and Astronautics. He has authored or coauthored nearly 60 research papers in international journals and conferences. His research interests focus on cooperative relay networks, MIMO communications systems, multiuser communication systems, satellite communication, hardware impairments, cognitive radio, NOMA technology and physical layer security. He also serves as an Editor on the Editorial Board for the EURASIP Journal on Wireless Communications and Networking. He was the Guest Editor for the special issue on Integration of Satellite-Aerial-Terrestrial Networks of Sensors, also the Guest Editor for the special issue on Recent Advances and Challenges of Satellite and Aerial Communication Networks of Electronics.

Dr. Guo has been the TPC member of many IEEE sponsored conferences, such as IEEE ICC, IEEE GLOBECOM and IEEE WCNC.